Chromium Hydrides and Dihydrogen Complexes in Solid Neon, Argon, and Hydrogen: Matrix Infrared Spectra and Quantum Chemical Calculations

Xuefeng Wang and Lester Andrews*

Department of Chemistry, University of Virginia, Charlottesville, Virginia 22904-4319

Received: September 6, 2002; In Final Form: November 12, 2002

Reactions of chromium atoms with molecular hydrogen are investigated through matrix-isolation infrared spectroscopy of products and complexes. Laser-ablated chromium atoms react with molecular hydrogen upon condensation in excess neon and argon and in pure hydrogen. The reaction products, CrH, $(H_2)CrH$, CrH_2, $(H_2)CrH_2$, and $(H_2)_2CrH_2$ are identified by isotopic substitution (D_2, HD, and H_2+D_2) and comparison with DFT (density functional theory) and MP2 calculations of vibrational fundamentals. The $(H_2)CrH$ complex with lower energy than CrH_3 is trapped and no band is observed for CrH_3. Reactions with H_2 and D_2 mixtures and with HD give different relative yields of the same mixed isotopic bands, which shows that exchange of dihydride and dihydrogen complex positions occurs in the energized $[CrH_4]$* intermediate in the formation of $(H_2)CrH_2$. The major bands at 1529.5 cm^{-1} for H_2 and 1112.2 cm^{-1} for D_2 in neon and at 1521.3 cm^{-1} in pure hydrogen and 1106.9 cm^{-1} in pure deuterium are due to $(H_2)_2CrH_2$ and $(D_2)_2CrD_2$, respectively, which is the most stable form for chromium hexahydride.

Introduction

In a previous paper we reported laser-ablated tungsten atom reactions with molecular hydrogen upon condensation in excess neon and argon.[1] The tungsten hydrides, WH, WH_2, WH_3, WH_4, and WH_6 were identified. The first successful synthesis of the highly fluxional WH_6 species is important to understanding the bonding of transition metal polyhydrides and polyhydrogen complexes. In this work, we investigate laser-ablated chromium atom reactions with molecular hydrogen.

The diatomic CrH molecule has been studied extensively both theoretically and experimentally.[2−8] It is well known that the ground electronic state for CrH is $^6\Sigma^+$, and recent high-resolution gas phase work provides a 1595.1 cm^{-1} vibrational fundamental.[8] The CrH molecule was prepared by reaction of thermal Cr and H atoms generated at 1700 and 2600 K and identified by ESR and optical spectroscopy in solid argon at 4 K; a 1548 cm^{-1} absorption was reported for the CrH molecule.[9] The CrH_2 molecule was also identified with both ESR and IR spectroscopy by Weltner et al.[9] Later, Margrave et al. reported the IR spectra of CrH_2 in krypton and argon matrices and assigned different frequencies. A bent structure with a bond angle of 118° was proposed based on the relative intensities of symmetric and antisymmetric stretching modes of CrD_2.[10] Soon afterward, Schaefer and co-workers reported ab initio calculations of CrH_2, which found a bent $^5B_2$ ground state.[11] The CrH_3 molecule has also been identified in inert gas matrices using the Cr atom photochemical reaction with H_2.[10] However, a recent theoretical study shows that the calculated ν_3 (e) mode of CrH_3 is substantially higher than reported,[10] and reassignment of this spectrum has been proposed.[12] Calculations have predicted that CrH_6 is stable in a distorted trigonal form, which is the global minimum for WH_6,[11−16] but that η^2-H_2 moieties are important here and the $(\eta^2\text{-}H_2)_3Cr$ complex is probably the lowest-energy structure for CrH_6.[13a]

Laser ablation is one of the most promising methods for vaporizing high-melting-point metals. With this approach reactive metal atoms are produced, which combine with H_2, and as a result, metal hydrides and hydrogen complexes can be synthesized.[17−19] Metal polyhydrides, ZrH_4, HfH_4, and TiH_4 with T_d structure,[20−22] and metal hydride hydrogen complexes, $(H_2)RhH_2$, $(H_2)RhH_3$, and $(H_2)AuH$, and $(H_2)AuH_3$ have been identified in neon and argon matrices by vibrational IR spectroscopy and reproduced by theoretical calculations.[23,24]

We present here a matrix isolation study of laser-ablated chromium atom reactions with H_2 in low-temperature matrices, which shows the importance of dihydrogen complexes. The chromium hydrides (CrH, CrH_2) and hydrogen complexes ($(H_2)CrH$, $(H_2)CrH_2$, and $(H_2)_2CrH_2$) are characterized by matrix infrared spectroscopy and quantum chemical calculations. The $(H_2)CrH$ species, which is lower in energy than CrH_3, is trapped instead of CrH_3, and likewise the $(H_2)CrH_2$ complex is produced instead of CrH_4. The higher bis-dihydrogen complex, $(H_2)_2CrH_2$, is formed predominantly in solid neon and pure hydrogen, and $(D_2)_2CrD_2$ in pure deuterium with no evidence for open CrH_6 or CrD_6 structures.

Experimental and Computational Methods

The experiments for reactions of laser-ablated chromium atoms with small molecules during condensation in excess argon and neon has been described in detail previously.[25−27] The Nd:YAG laser fundamental (1064 nm, 10 Hz repetition rate with 10 ns pulse width) was focused (10 cm f.l. lens) onto a rotating chromium target (Johnson Matthey). The laser energy was varied from 10 to 30 mJ/pulse at the sample. Laser-ablated chromium atoms were co-deposited with 0.2 to 2% hydrogen (Matheson) in excess neon or argon and with pure hydrogen or deuterium onto a 3.5 K CsI cryogenic window at 2−4 mmol/h for 1 h. Isotopic D_2 (Liquid Carbonic), HD (Cambridge Isotopic Laboratories), and selected mixtures were used in different experi-

* Corresponding author. E-mail: lsa@virginia.edu

10.1021/jp026930h CCC: $25.00
Published on Web 01/01/2003

TABLE 1: Infrared Absorptions (cm^{-1}) Observed from Reactions of Laser-Ablated Chromium and Dihydrogen in Excess Argon, Neon, Pure Hydrogen, and Deuterium

argon			neon			pure solid		identification
H_2	HD	D_2	H_2	HD	D_2	H_2	D_2	
						3757.4	2710.7	$(H_2)CrH$
1650.9	1642	1188.9		1641.8				CrH_2
1635.6		1176.4						unknown[a]
1614.5	1185	1166.8	1627.7	1186.7	1180.0			CrH_2
1603.3	1603.3, 1158.7	1158.7						CrH
1581.2	1623.9 1171.9	1139.4						(H_2)- -CrH_2
						1578.4	1144.8	$(CrH_2)_2$
1561.5		1126.8						$(H_2)CrH$ site
1547.5	1546.6 1114.8	1114.4	1561.8	1558.9 1123.4	1122.5	1555.4	1119.0	$(H_2)CrH$
1525.4[b]	1524, 1108 1576, 1133	1106.9[c]	1529.5	1530.9, 1113.0, 1583.4, 1137.1	1112.2	1521.3	1106.9	$(H_2)_2CrH_2$
			1525.8	1576.4, 1133.4 1524.1, 1108.2	1107.6			$(H_2)CrH_2$
			1377.7	1337.2	994.2	996.7		Cr_xH_y
1332.4		971.8	1335.0	1333.2, 973.0	971.6	1336.6	971.2	$(CrH_2)_2$
1238.4		903.8	1243.5		909.8	931.2		$(CrH_2)_2$
			1299.9	967.4	950.0	1299	950.6	Cr_xH_y
1210.4		882.9	1215.7		884.5	847.4		Cr_xH_y
			1165.9		856.8			Cr_xH_y

[a] Weak, increased on photolysis. [b] Annealing produced sharp peaks at 1519.3 and 1509.5 cm^{-1}. [c] Annealing produced sharp peaks at 1106.4 and 1098.5 cm^{-1}.

TABLE 2: Calculated Electronic States, Relative Energies, and Geometries for Chromium Hydrides and Hydrogen Complexes

species	state	relative energy (kcal/mol)	geometries (Å, deg)
		B3PW91/6-311++G(d,p)/SDD	
CrH	$^6\Sigma^+$	0.0	CrH: 1.647
CrH_2	$^5B_2$	0.0	CrH: 1.637; HCrH: 111.3
$(H_2)CrH$	$^6A_1$	0.0	CrH: 1.671; CrH′: 2.064; H′H′: 0.756
CrH_3	$^4A_1$	20.5	CrH: 1.605; HCrH: 106.6
$(H_2)CrH_2$	$^5A_1$	0.0	CrH: 1.701; CrH′: 1.868; H′H′: 0.792; HCrH: 171.8
CrH_4	$^3A_1$	25.5	CrH: 1.582
$(H_2)_2CrH_2$	$^5A_1$	0.0	CrH: 1.696; CrH′: 1.884; HH: 0.786; HCrH: 180.0
$Cr(\eta^2\text{-}H_2)_3$	$^1A_1$	53.3	CrH; 1.601; CrH′: 1.625; HH′: 0.973; HCrH: 66.1; H′CrH′: 112.8
Cr_2H_2	$^{11}B_u$	0.0	CrH: 1.806, 1.807, CrHCr: 101.9
Cr_2H_4	^9A_g	0.0	HCr: 1.665; Cr−H′: 1.878, 1.740
		B3LYP/6-311++G(d,p)/SDD	
CrH_2	$^5B_2$		CrH: 1.641; HCrH: 112.0
$(H_2)CrH_2$	$^5A_1$		CrH: 1.709; CrH′: 1.924, H′H′: 0.779; HCrH: 176.5
$(H_2)_2CrH_2$	$^5A_1$		CrH: 1.701; CrH′: 1.912; H′H′: 0.778; HCrH: 180.0
		BPW91/6-311++G(d,p)/all electron	
CrH_2	$^5B_2$		CrH: 1.639; HCrH: 109.8
		MP2/6-311++G(d,p)/SDD	
CrH_2	$^5B_2$	0.0	CrH: 1.614; HCrH: 113.6
$(H_2)CrH$	$^6A_1$	0.0	CrH: 1.664; CrH′: 1.989; HH: 0.758
CrH_3	$^4A_1$	27.2	CrH: 1.589; HCrH: 106.6
$(H_2)CrH_2$	$^5A_1$	0.0	CrH: 1.698; CrH′: 2.002; H′H′: 0.759; HCrH: 176.1
CrH_4	$^3A_1$	170.2	CrH: 1.622
$(H_2)_2CrH_2$	$^5A_1$	0.0	CrH: 1.622; CrH′: 1.667; H′H′: 0.809; HCrH: 180.0
CrH_6	$^1A_1$	41.0	CrH: 1.465; CrH′: 1.499; HH′: 1.636; HCrH: 67.0; H′CrH′: 115.5

ments. FTIR spectra were recorded at 0.5 cm^{-1} resolution on a Nicolet 750 with 0.1 cm^{-1} accuracy using an MCTB detector. Matrix samples were annealed at different temperatures, and selected samples were subjected to broadband photolysis by a medium-pressure mercury arc lamp (Phillips, 175W) with globe removed.

DFT (density functional theory) and MP2 (Møller−Plesset) calculations of chromium hydrides and chromium-hydride−hydrogen complexes are given for comparison. The Gaussian 98 program[28] was employed to calculate the structures and frequencies of expected molecules. The 6-311++G(d,p) basis set for hydrogen atom and the SDD pseudopotential and basis for chromium atom were used.[29,30] All the geometrical parameters were fully optimized with the B3PW91 and B3LYP density functionals and calculations at the MP2 level of theory.[31−33] Analytical B3PW91, B3LYP and MP2 vibrational frequencies were obtained at the optimized structures. The computed geometry parameters, relative energies, and frequencies, intensities, and isotopic frequency ratios are summarized in Tables 2 and 3.

TABLE 3: Calculated Vibrational Frequencies and Intensities for Chromium Hydrides and Dihydrogen Complexes

species	state	frequencies, cm^{-1} (symmetry, intensities, km/mol)
		B3PW91/6-311++G(d,p)/SDD
CrH	$^6\Sigma^+$	1642.0(210)
CrH_2	$^5B_2$	1692.2(a_1,80); 1676.5(b_2,295); 614.7(a_1,131)
$(H_2)CrH$	$^6A_1$	4061.6(a_1,25); 1622.7(a_1,219); 859.1(b_2,9); 484.8(a_1,1); 343.5(b_1,85); 325.1(b_2,109)
CrH_3	$^4A_1$	1761.2(a_1,16); 1760.6(e,210×2); 595.9(e,45×2); 482.4(a_1,234)
$(H_2)CrH_2$	$^5A_1$	3660.1(a_1,64); 1679.9(a_1,1); 1523.5(b_2,1041); 1346.4(b_2,38); 776.3(a_1,8); 681.8(a_2,0); 500.6(b_1,246); 423.0(a_1,315); 254.8(b_2,115)
CrH_4	$^3A_1$	1830.5(t_2,159×3); 1799.4(a_1,0); 708.2(e,0×2); 536.6(t_2,134×3)
$(H_2)_2CrH_2$	$^5A_1$	3764.7(a_1,0); 3751.9(b_1,128); 1675.7(a_1,0); 1543.8(b_2,738); 1322.7(a_2,0); 1308.9(b_2,60); 799.2(b_1,0); 781.9(a_1,0); 628.6(b_2,0); 599.3(a_2,0); 494.8(a_1,213); 276.1(a_2,0); 247.9(a_1,0); 215.2(b_1,356); 188.2(b_2,97)
$Cr(\eta^2\text{-}H_2)_3$	$^1A_1$	2163.7(a_1,0); 2074.5(e,425×2); 1932.4(a_1,11); 1930.6(e,172×2); 1029.5(a_1,12); 850.1(e,522×2); 773.3(a_1,66); 742.4(e,71×2); 614.4(e,47×2); 481.2(a_2,0)
Cr_2H_2	$^{11}B_u$	1233.2(a_g, 0); 1097.4(b_u, 191); 894.7(b_u, 87); 645.1(a_g, 0); 438.5(a_u, 94); 236.6(a_g, 0)
Cr_2H_4	^9A_g	1688.1(a_g, 0); 1672.5(b_u, 623); 1364.8(b_u, 908), 1348.0(a_g, 0); 1155.1(a_g, 0); 1134.9(b_u, 444); 473.5(a_u, 256); 424.4(a_g, 0); 339.7(b_u, 319); ...
		B3LYP/6-311++G(d,p)/SDD
CrH_2	$^5B_2$	1698.4(a_1, 88); 1681.8(b_2, 317), 630.3(a_1, 121)
$(H_2)CrH_2$	$^5A_1$	3837.6(a_1, 47); 1678.2(a_1, 4); 1515.2(b_2, 1086); ...0.408.6(a_1, 351); 265.6(b_2, 82)
$(H_2)_2CrH_2$	$^5A_1$	3860.0(a_1, 0); 3849.5(b_1, 101); 1670.5(a_1, 0); 1536.9(b_2, 785); ...0.234.7(a_1, 2); 240.8(b_2, 85)
		BPW91/6-311++G(d,p)/all electron
CrH_2	$^5B_2$	1689.6(a_1, 78); 1682.6(b_2, 242); 584.6(a_1, 120)
		MP2/6-311++G(d,p)/SDD
CrH_2	$^5B_2$	1756.3(a_1,249); 1748.5(b_2,618); 561.9(a_1,106)
$(H_2)CrH$	$^6A_1$	4189.2(a_1,22); 1706.1(a_1,256); 1020.9(b_2,11); 575.3(a_1,4); 376.6(b_2,120); 354.5(b_1,99)
CrH_3	$^4A_1$	1894.3(e,134×2); 1772.7(a_1,7); 927.7(e,1263×2); 466.6(a_1,299)
$(H_2)CrH_2$	$^5A_1$	4200.1(a_1,1); 1751.5(a_1,11); 1571.2(b_2,1003); 1100.2(b_2,13); 555.8(a_1,66); 504.0(a_2,0); 481.6(b_1,331); 477.3(a_1,335); 341.9(b_2,26)
$(H_2)_2CrH_2$	$^5A_1$	4086.9(b_1,13); 4084.8(a_1,0); 1755.9(a_1,0); 1597.4(b_2,881); 1270.5(a_2,0); 1255.6(b_2,45); 754.8(b_1,3); 672.9(a_1,0); 581.3(b_2,0); 542.6(a_2,0); 476.6(a_1,269); 449.1(b_1,347); 435.2(a_2,0); 266.3(b_2,84); 223.6(a_1,5)
CrH_6	$^1A_1$	2480.8(a_1,4); 2322.9(e,120×2); 2185.7(a_1,94); 2128.1(e,114×2); 1403.5(a_1,112); 1165.1(e,175×2); 1069.2(e,100×2); 886.3(a_2,0); 722.4(a_1,38); 587.2(e,24×2)

Results

Infrared spectra of reaction products recorded in argon, neon, and pure hydrogen and deuterium at 3.5 K are presented, and calculations with DFT and MP2 were used to support the product identifications.

Argon Matrix Spectra. Figure 1 shows the infrared spectra of Cr−H stretching regions for Cr reactions with 5% H_2 in excess argon. Two bands at 1614.5 and 1650.9 cm^{-1} due to CrH_2 in argon were observed, which are basically the same as the frequencies reported by Xiao et al.[10] A new band appeared at 1547.5 cm^{-1} on deposition and increased greatly on annealing.

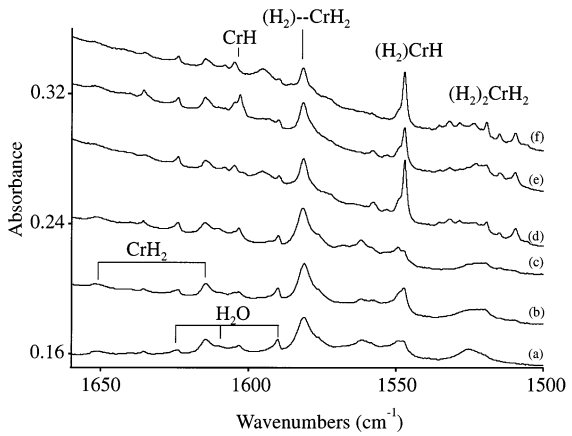

Figure 1. Infrared spectra of laser-ablated chromium atom and H_2 (4%) reaction products in an argon matrix in the 1660−1500 cm^{-1} region: (a) 60 min deposition at 3.5 K, (b) after annealing to 15 K, (c) after 10 min broadband photolysis, (d) after annealing to 25 K, (e) after 10 min broadband photlysis, and (f) after annealing to 30 K.

This band decreased in intensity on broadband photolysis, and a very weak band at 1603.3 cm^{-1} increased. Deuterium counterparts for these two bands appeared at 1114.4 and 1158.7 cm^{-1} (Figure 2). Experiments with HD and H_2+D_2 gave exactly the same 1603.3 and 1158.7 cm^{-1} bands, but the 1547.5 and 1114.4 cm^{-1} bands show wavenumber shifts of several tenths, as shown in Figure 3. A strong, broad band at 1581.2 cm^{-1} and a deuterium counterpart at 1139.4 cm^{-1} were also observed on deposition. Mixed H_2+D_2 experiments gave approximately the same bands, but HD shifted two bands to 1623.9 and 1171.9 cm^{-1}, respectively.

Neon Matrix Spectra. Figure 4 reveals reaction products in neon. Strong 1525.8 cm^{-1} and weak 1561.8 and 1627.7 cm^{-1}

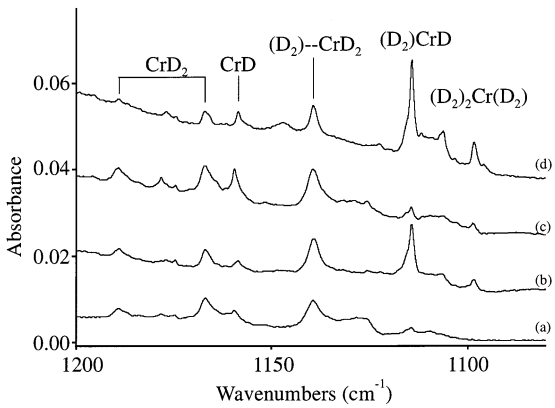

Figure 2. Infrared spectra of laser-ablated chromium and D_2 (4%) reaction products in argon an matrix in the 1200−1080 cm^{-1} region: (a) 60 min deposition at 3.5 K, (b) after annealing to 18 K, (c) after 10 min broadband photolysis, and (d) after annealing to 25 K.

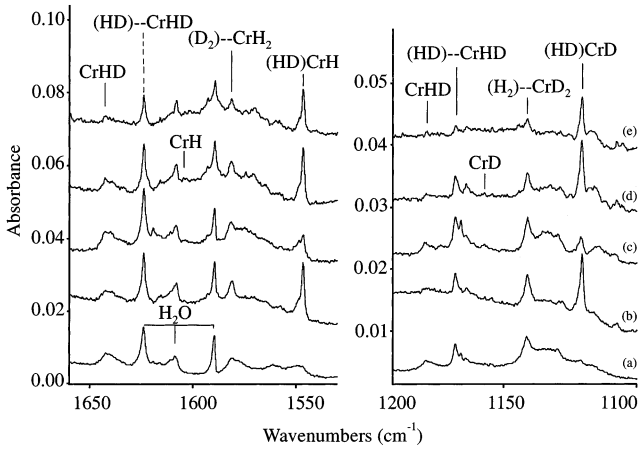

Figure 3. Infrared spectra of laser-ablated chromium and HD (7%) reaction products in an argon matrix in the 1660−1530 cm^{-1} and 1200−1100 cm^{-1} regions: (a) 70 min deposition at 3.5 K, (b) after annealing to 20 K, (c) after 10 min broadband photolysis, (d) after annealing to 25 K, and (e) after annealing to 30 K.

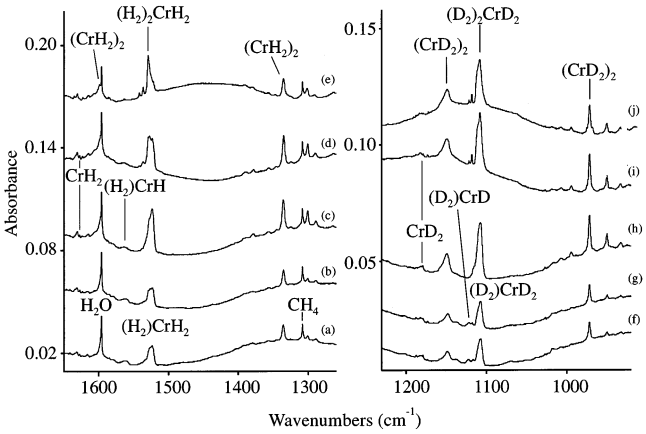

Figure 4. Infrared spectra of laser-ablated chromium and H_2 (5%) reaction products in a neon matrix in the 1640−1280 cm^{-1} region: (a) 60 min deposition at 3.5 K, (b) after annealing to 7 K, (c) after 10 min broadband photolysis, (d) after annealing to 9 K, (e) after annealing to 12 K, and infrared spectra of for laser-ablated chromium and D_2 (5%) reaction products in a neon matrix in the 1220−920 cm^{-1} region, (f) 60 min deposition at 3.5 K, (g) after annealing to 7 K, (h) after 10 min broadband photolysis, (i) after annealing to 9 K, and (j) after annealing to 12 K.

bands were observed in the Cr−H stretching region. Broadband photolysis increased the 1525.8 cm^{-1} band 3-fold and annealing increased a sharp feature at 1529.5 cm^{-1}. The deuterium counterparts for these bands are at 1107.6 and 1112.2 cm^{-1}, respectively. The HD spectrum reveals new bands at 1576.4 cm^{-1} in the upper region and at 1133.4 cm^{-1} in the lower region and weaker 1524.1 and 1108.2 cm^{-1} bands (Figure 5). The mixed H_2+D_2 experiment reveals a similar spectrum with stronger bands at 1523.6 and 1108.0 cm^{-1} and weaker absorptions at 1576.4 and 1133.4 cm^{-1} (Figure 6). Finally experiments were done with lower laser energies, and two spectra are compared from three experiments with different laser energies. The spectra in Figure 7 show that absorptions in the 1400−1100 cm^{-1} region are higher order in laser energy than bands in the 1500−1700 cm^{-1} region.

Deuterium and Hydrogen Matrix Spectra. Pure D_2 was used as both reagent and matrix in this work, and simple reaction product absorptions were recorded. As shown in Figure 8, the strongest band at 1106.9 cm^{-1} appeared on deposition, increased on annealing, and decreased on photolysis. However a sharp

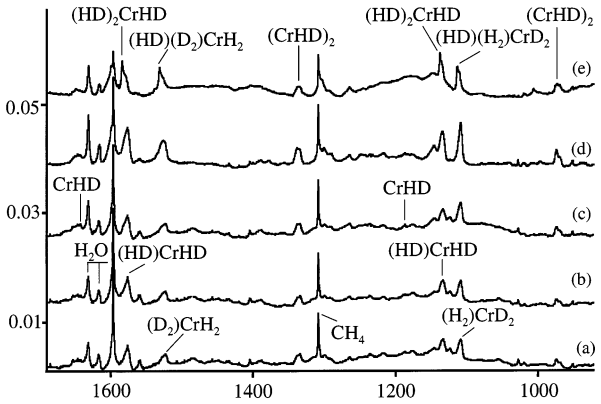

Figure 5. Infrared spectra of laser-ablated chromium and HD (5%) reaction products in a neon matrix in the 1690−920 cm^{-1} region: (a) 70 min deposition at 3.5 K, (b) after annealing to 7 K, (c) after 10 min $\lambda > 380$ nm photolysis, (d) after 10 min $\lambda > 240$ nm photolysis, and (e) after annealing to 13 K.

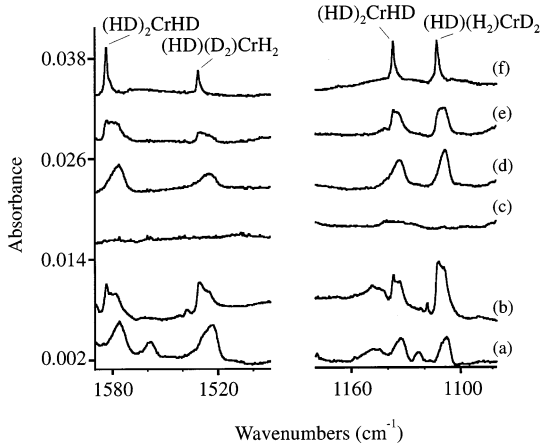

Figure 6. Infrared spectra in the 1590−1490 and 1180−1080 cm^{-1} regions for laser-ablated chromium reaction products with H_2+D_2 mixtures and HD in excess neon: (a) 70 min deposition of 4% H_2+D_2 in neon at 3.5 K, (b) after photolysis and annealing to 13 K, (c) 70 min deposition with 5% HD in neon at 3.5 K using lower laser energy than the experiment reported in Figure 5, (d) after 25 min photolysis with 240−380 nm radiation, (e) after annealing to 11 K, and (f) after annealing to 12 K.

band at 1119.0 cm^{-1} decreased markedly on broadband photolysis and tracked with a sharp weaker 2710.6 cm^{-1} peak, both increasing slightly on 8 K annealing. Bands observed at 1144.8 and 971.2 cm^{-1} on deposition decrease slightly on photolysis and increase slightly on annealing. Finally, a new photosensitive 2870 cm^{-1} absorption is observed in pure deuterium experiments independent of the laser-ablated metal.[17,19,23,24] This photosensitive 2870 cm^{-1} band is, we believe, due to a $(D_2)_nD^+$ species, which will be described in a later publication.

Pure H_2 was co-deposited with laser-ablated chromium using half the laser energy employed for D_2, and the product bands at 1555.4 and 1521.3 cm^{-1} are illustrated in Figure 9a. Photolysis broadened the latter and decreased the former band, and 6.5 K annealing sharpened these bands. Additional weaker bands are listed in Table 1. A similar experiment performed with pure HD gave new absorptions 1574.2, 1554.6, 1522.8, 1131.7, 1120.8, and 1107.9 cm^{-1}, and the Cr−H stretching region is shown in Figure 9d. Photolysis produced new bands at 1580.0, 1524.6, 1135.6, and 1109.2 cm^{-1}, and subsequent annealing to 6.5 K destroyed these latter bands and increased the 1522.8 and 1107.9 cm^{-1} absorptions. Mixed H_2, D_2 samples with 35, 50, 65, and 85% H_2 were co-deposited with Cr, and

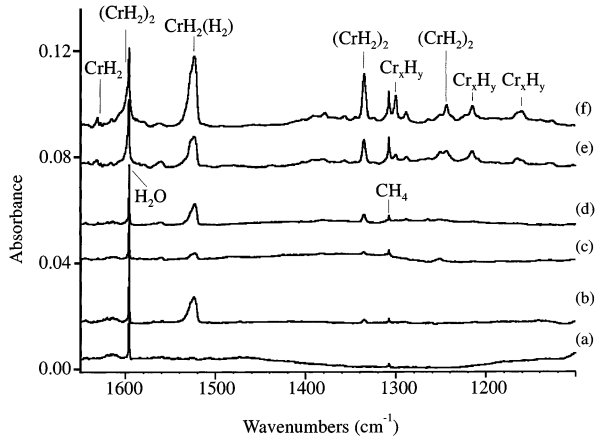

Figure 7. Infrared spectra in the 1650−1100 cm^{-1} region for laser-ablated chromium reaction products with 5% H_2 in neon using different laser energies at the sample: (a) ablation at 10 mJ/pulse for 60 min with deposition at 3.5 K, (b) after $\lambda > 240$ nm photolysis, (c) ablation at 15 mJ/pulse for 60 min with deposition at 3.5 K, (d) after 240−380 nm photolysis, (e) ablation at 30 mJ/pulse for 60 min with deposition at 3.5 K, and (f) after $\lambda > 240$ nm photolysis.

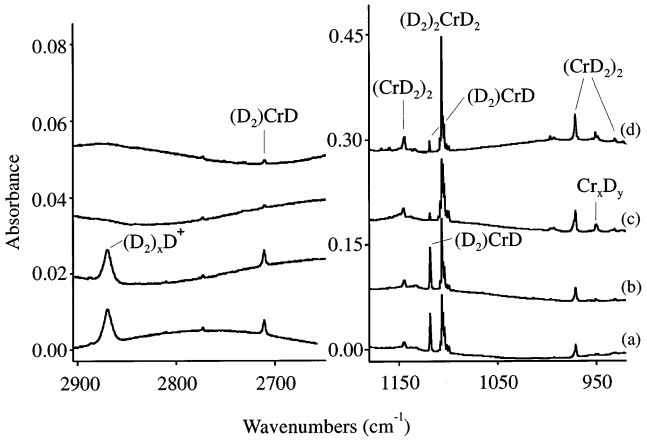

Figure 8. Infrared spectra in the 2910−2650 and 1180−920 cm^{-1} regions for laser-ablated chromium and D_2 reaction products in a deuterium matrix: (a) deposition with pure D_2 at 3.5 K for 25 min, (b) after annealing to 7 K, (c) after 10 min broadband photolysis, and (d) after annealing to 8 K.

new product bands were observed with different relative intensities. The 85% H_2, 15% D_2 sample spectrum is shown in Figure 9g: the strongest feature at 1523.5 cm^{-1} increased with increasing H_2 percentage and new 1525.4 and 1521.9 cm^{-1} satellite absorptions increased on photolysis and decreased on annealing, which favored the 1523.5 cm^{-1} feature. Weaker absorptions were observed at 1573.9 and 1553.2 cm^{-1}: photolysis increased the 1573.9 cm^{-1} band and produced a new 1579.3 cm^{-1} peak, which was stronger with increasing D_2 percentage. Subsequent photolysis and annealing cycles (Figure 9j,k) had the same effect. Similar deuterium counterpart absorptions were observed at 1106.7 cm^{-1} with satellites at 1108.4 and 1105.1 cm^{-1} and weaker bands at 1131.5 and 1120.3 cm^{-1}. In addition, a photosensitive band is observed at 3972 cm^{-1} in pure hydrogen, which is due to $(H_2)_nH^+$.

Calculations. DFT and MP2 calculations are done for chromium hydrides and hydrogen complexes, and the calculated results are summarized in Tables 2 and 3. The ground state of CrH is predicted to be $^6\Sigma^+$ and the 1.647 Å bond length and 1642.0 cm^{-1} Cr−H stretching frequency calculated at the B3PW91/6-311++G**/SDD level of theory are close to the latest gas-phase experimental values of 1.655 Å and 1656.1 cm^{-1}, respectively.[8] The geometry and frequency of CrH have been extensively explored with MCSCF/MRCI and other theoretical methods, and our DFT calculations are in excellent agreement.[8]

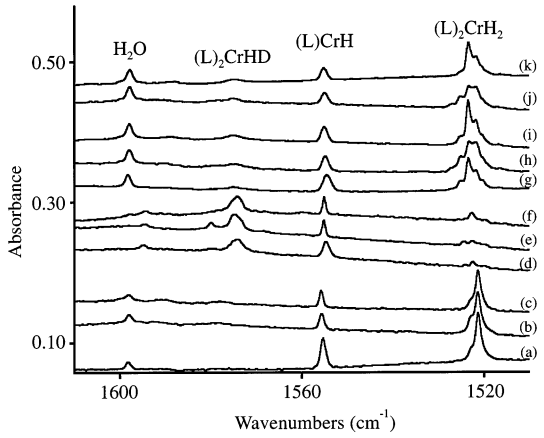

Figure 9. Infrared spectra in the 1610−1510 cm^{-1} region for laser-ablated chromium reaction products in solid hydrogen: (a) deposition with pure H_2 at 3.5 K for 25 min, (b) after 10 min broadband photolysis, (c) after annealing to 6.5 K, (d) deposition with pure HD at 3.5 K for 25 min, (e) after 10 min broadband photolysis, (f) after annealing to 6.5 K, (g) deposition with 85% H_2 and 15% D_2 at 3.5 K for 25 min, (h) after 10 min broadband photolysis, (i) after annealing to 6.5 K, (j) after 10 min broadband photolysis, and (k) after annealing to 7 K. (L) denotes an isotopic dihydrogen ligand.

When one H_2 molecule is added to CrH, the coplanar (H_2)-CrH complex with $^6A_1$ ground state is predicted to be the energetically lowest-lying isomer. In this complex the Cr−H bond is elongated by 0.024 Å and the Cr−H stretching frequency is red-shifted by 20 cm^{-1} compared to free diatomic CrH (B3PW91 calculation). At the same level pyramidal CrH_3 with the $^4A_1$ ground state is 20.5 kcal/mol higher in energy than (H_2)CrH, and the Cr−H bond length for CrH_3 is much shorter than that of diatomic CrH. As a result the Cr−H stretching mode lies more than 100 cm^{-1} higher.[12] Similar results were found with MP2 calculations. This suggests that (H_2)CrH should be formed instead of CrH_3.

As for the CrH_2 molecule, the geometries, electronic states, and vibrational frequencies have been investigated extensively with CISD and CCSD(T) methods, and the bent $^5B_2$ electronic ground state was predicted.[11] Our DFT and MP2 calculations are in excellent agreement with previous theoretical studies. Two conformers, the $(H_2)CrH_2$ complex and CrH_4 tetrahydride, are considered when H_2 is added to CrH_2. The high-spin coplanar $(H_2)CrH_2$ complex with the $^5A_1$ ground state lies lower in energy at both DFT and MP2 levels of theory, which is in accord with CCSD(T) calculations.[11b] It is interesting to note that the geometry of the CrH_2 moiety in $(H_2)CrH_2$ is changed dramatically from free CrH_2 by coordination of H_2: the Cr−H bond is elongated by 0.06 Å and the HCrH bond angle is increased from 111.3° to 171.7° based on DFT predictions. The H−H distance 0.792 Å is longer than free H_2 and H−H (0.765 Å) in (H_2)-CrH, indicating that the interaction between H_2 and CrH_2 is very strong. The optimization of $(H_2)CrH_2$ on the triplet potential energy surface leads to the $^3A_2$ tetrahydride CrH_4, which is 25.5 kcal/mol higher in energy, and the Cr−H stretching frequency predicted at 1830.2 cm^{-1} is 300 cm^{-1} higher than that in the $^5A_1$ $(H_2)CrH_2$ molecule. Note that MP2 calculations are in very good agreement (Table 2). This energy separation is 38.5 kcal/mol at the CCSD level.[11b]

Similar higher chromium bis-dihydrogen complexes are calculated as two H_2 moieties are associated with CrH_2. The

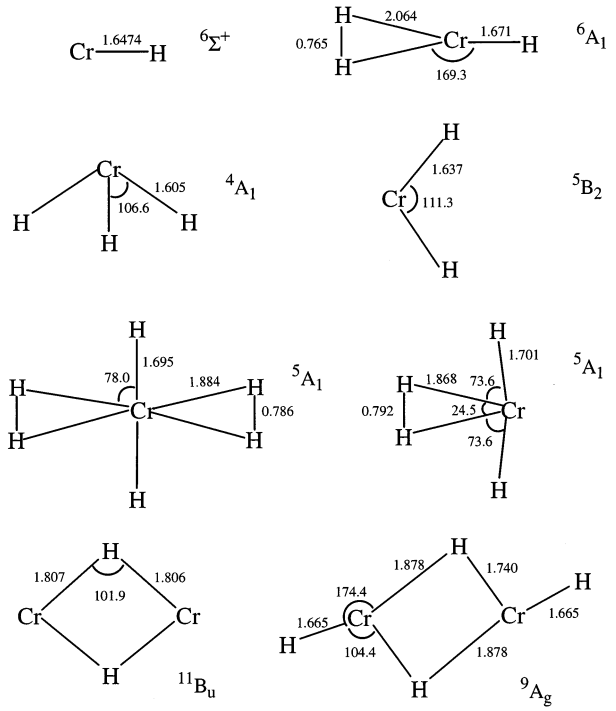

Figure 10. Structures calculated using B3PW91 and 6-311++G(d,p) for H and SDD for Cr. Bond lengths in Å; angles in deg.

global minimum appears to be $(H_2)CrH_2(H_2)$ ($^5A_1$) with C_{2v} symmetry (slightly distorted from the planar D_{2h} structure) at both the B3PW91 and MP2 levels of theory. An all-electron calculation (B3PW91) gave virtually the same minimum energy structure and frequencies. This result is not in agreement with early QCISD(T) calculations, where $Cr(\eta^2\text{-}H_2)_3$ with C_{3v} symmetry was proposed as the energetically lowest-lying species.[13b] As shown in Figure 10 the H−Cr−H linkage in $(H_2)CrH_2(H_2)$ is linear and two H_2 molecules are coordinated on opposite sides of Cr as ligands. On the singlet potential energy, surface optimization of this molecule with DFT leads to a C_{3v} $Cr(H_2)_3$ complex, which is 53.3 kcal/mol higher in energy. This strong η^2-complex is analogous to the distorted C_{3v} prism structure calculated[1,13−16] for WH_6, but the H−H bonds are substantially shorter (0.973 Å). However MP2 calculations find the trigonal classical hexahydride CrH_6 (analogous to WH_6)[1,14] with shorter Cr−H bonds (1.465, 1.499 Å) and longer H−H distance (1.636 Å), which is 41.0 kcal/mol higher in energy than $(H_2)_2CrH_2$ (Table 2). This suggests that the $(H_2)_2CrH_2$ complex should be observed instead of CrH_6.

In view of the known tendencies of MP2 to overestimate and DFT to underestimate the interaction between the dihydrogen molecule and metal complexes,[34,35] we also employ the B3LYP functional for comparison of $(H_2)CrH_2$ and $(H_2)_2CrH_2$. The results are listed in Tables 2 and 3.

Finally, DFT calculations were done on two dichromium species, namely dimers of CrH and CrH_2. The distorted high-spin structures shown in Figure 10 were obtained.

Discussion

The chromium hydride products and complexes will be identified from isotopic substitution and from the comparison of results from solid argon, neon, hydrogen, and deuterium, and quantum chemical calculations.

CrH and (H_2)CrH. A weak absorption at 1603.3 cm^{-1} is observed after initial co-deposition of laser-ablated chromium atoms with H_2 in excess argon at 3.5 K (Figure 1). This band increased slightly on first annealing and then decreased on further annealing, but increased markedly on broadband photolysis. The D_2 counterpart for this band at 1158.7 cm^{-1} gives H/D isotopic frequency ratios of 1.3837. With HD and H_2+D_2, these two bands are in exactly the same position as in the separate H_2 and D_2 experiments. The isotopic doublet and H/D ratio are appropriate for the diatomic molecule CrH. This absorption is in good agreement with the recent gas-phase fundamental frequency of 1595.1 cm^{-1}.[8] Our calculations predicted the harmonic diatomic CrH stretching frequency at 1642.0 cm^{-1} (B3PW91), which is higher than recent MRCI calculations[8] but in good agreement with experiment. The CrH molecule was not trapped in solid neon owing to formation of the (H_2)CrH complex.

The 1547.5 cm^{-1} argon matrix band (Figure 1) appeared on deposition, increased markedly on annealing, but decreased on broadband photolysis and restored the original 1603.3 cm^{-1} absorption. The band shifts to 1114.3 cm^{-1} with D_2 in argon, giving the 1.3888 H/D isotopic ratio. In HD experiments the upper H band is red-shifted 0.5 cm^{-1} while the lower D band is blue-shifted 0.4 cm^{-1}, indicating Cr−H (D) stretching vibrations slightly perturbed by another HD molecule. Experiments with H_2+D_2 gave two broad bands centered at 1546.7 and 1114.8 cm^{-1}, where each band is possibly due to two overlapped absorptions. The above absorptions must be considered for the (H_2)CrH complex: the broad bands in H_2+D_2 are due to (H_2)CrH and (D_2)CrH in the upper region and (H_2)CrD and (D_2)CrD in the lower region. The H_2 moiety in (H_2)CrH is eliminated on broadband photolysis, and as a result the band due to isolated CrH is produced. The 1548 cm^{-1} band first assigned by Weltner et al.[9] to CrH must be reassigned to the (H_2)CrH complex, which is red-shifted 55.8 cm^{-1} from isolated CrH.

The assignment of (H_2)CrH is further supported by neon matrix observations of weak bands at 1561.8 cm^{-1} with H_2 and 1122.5 cm^{-1} with D_2 (1.3888 ratio). Counterparts for these bands in HD are observed at 1558.9 and 1123.4 cm^{-1}, and with H_2+D_2 at 1558.2 and 1123.1 cm^{-1}, respectively. Clearly due to the perturbation of H_2, the small red-shift for the upper Cr−H stretching and blue-shift for Cr−D stretching modes are also observed in neon. Note the fate of this band in neon is quite unlike that in argon: the neon matrix bands reduced on annealing, decreased on photolysis, and never restored on further annealing.

In pure deuterium isolated CrD is not observed, but a strong 1119.0 cm^{-1} band appeared on deposition, decreased markedly on broadband photolysis, and increased slightly on further annealing (Figure 8). The pure hydrogen counterpart at 1555.4 cm^{-1} (Figure 9) defines a 1.3900 H/D ratio. These bands between the argon and neon matrix values are assigned to (H_2)CrH and (D_2)CrD. The pure HD experiment gave sharp new bands at 1554.6 and 1120.8 cm^{-1} (ratio 1.3870) for (HD)CrH and (HD)CrD, and mixed H_2/D_2 experiments gave broader bands at 1553.2 and 1120.3 cm^{-1}. The formation of a high yield of (D_2)CrD in pure deuterium made possible the observation of a weak associated 2710.6 cm^{-1} band for the D−D stretching mode.

B3PW91 and MP2 calculations were done for (H_2)CrH and the frequencies are listed in Table 3. The strongest mode for this molecule is (H_2)Cr−H stretching computed at 1622.7 cm^{-1} and (D_2)Cr−D stretching at 1157.8 cm^{-1} (B3PW91). Furthermore the (D_2)Cr−H stretching mode is predicted to red-shift 0.5 cm^{-1} and (H_2)Cr−D stretching to blue-shift 0.5 cm^{-1}, which

reproduce the observed values very well. Furthermore, the (H_2)-CrH complex is predicted to red-shift the Cr−H fundamental 19.3 cm^{-1}, which is less than the observed 55.8 cm^{-1} red-shift. Finally the 2710.6 cm^{-1} band for the D−D stretching mode in (D_2)CrD is lower than predicted by DFT. It appears that DFT underestimates the strength of the D_2−CrD interaction.

CrH_2 and $(H_2)CrH_2$. The absorptions due to CrH_2 in argon at 1614.5 and 1650.9 cm^{-1} are basically the same as the frequencies reported by Xiao et al.[10] Hence, the bands assigned to CrH_2 by Van Zee et al.[9] are probably due to a weak (H_2)−CrH_2 complex. Only the stronger antisymmetric Cr−H stretching frequency for CrH_2 is observed in solid neon, at 1627.7 cm^{-1}, which is a reasonable matrix shift;[36] this band is displaced to 1180.0 cm^{-1} with D_2. The HD spectrum gave two new sharp bands at 1641.8 and 1186.7 cm^{-1}, which increased together on $\lambda > 380$ nm photolysis (Figure 5) and characterize this CrH_2 vibration. Our B3PW91 calculations predict a stronger b_2 mode at 1676.5 cm^{-1} and a weaker a_1 mode at 1692.2 cm^{-1}: the same systematic overestimation of frequencies was found for CrH. However the MP2 method gives higher frequencies compared to DFT calculations, but the CCSD frequencies[11a] are nearly the same as DFT for the $^5B_2$ ground-state molecule. These CrHD absorptions in neon are 14.1 and 6.7 cm^{-1} above the strong b_2 CrH_2 and CrD_2 bands, which agree with 13 and 6 cm^{-1} differences calculated by CCSD[11a] (the analogous B3PW91 differences are 7.6 and 2.6 cm^{-1}). Excellent agreement between the observed CrH_2, CrHD, and CrD_2 band positions and theoretical predictions supports the assignment to isolated CrH_2.

The strong band at 1581.2 cm^{-1} observed in solid argon after deposition increased slightly on annealing to 20 K, but decreased on further annealing to 30 K. This absorption shifts to 1139.4 cm^{-1} with D_2 in argon, and the H/D isotopic frequency ratio is 1.3877. An experiment with $H_2 + D_2$ gave two broad bands; the upper band is 0.3 cm^{-1} red-shifted and the lower band is 0.2 cm^{-1} blue-shifted from the bands observed in H_2 and D_2, which indicate that the mode is perturbed by a hydrogen molecule. In the HD experiment a new band at 1171.9 cm^{-1} shows the same behavior as the 1581.4 and 1139.5 cm^{-1} absorptions in this experiment and is due to one CrHD counterpart where the other CrHD absorption is masked by water at 1623.9 cm^{-1}. These bands are due to a CrH_2 vibration and are assigned to a weak (H_2)−CrH_2 complex involving the CrH_2 ($^5B_2$) ground state. Observation of the 1581.4 and 1139.5 cm^{-1} bands for (D_2)−CrH_2 and (H_2)−CrD_2, respectively, in the HD experiment shows that an activated intermediate is involved that allows exchange of hydride and dihydrogen positions.

The strongest solid neon product band in this region appears lower at 1525.8 cm^{-1}. The band doubled on photolysis and shifts to 1107.6 cm^{-1} with D_2 (Figure 4), giving a similar 1.3776 H/D isotopic frequency ratio and reveals new HD counterparts at 1576.4 and 1133.4 cm^{-1} (Figure 5). These observations characterize a CrH_2 vibration. Ma and co-workers found the strong $^5A_1$ $(H_2)CrH_2$ complex to be the most stable CrH_4 species and predicted the strongest infrared band, the antisymmetric CrH_2 stretching mode, to red-shift 67 cm^{-1} from the $^5B_2$ ground state CrH_2 (TZP CISD level).[11b] Our 1525.8 cm^{-1} neon matrix band is assigned to this strong $^5A_1$ $(H_2)CrH_2$ complex, which is 102 cm^{-1} below isolated CrH_2 in solid neon. The slightly shifted 1581.2 cm^{-1} band in solid argon is probably due to a weak (H_2)−CrH_2 complex with the $^5B_2$ ground state. Xiao et al.[10] first proposed that the "b" satellite bands for CrH_2 were due to $(H_2)CrH_2$. However Ma et al. find that the $^5B_2$ ground CrH_2 state is slightly repulsive for attachment of one dihydrogen ligand,[11b] hence our designation is a weak complex.

Note that H_2+D_2 experiments give the strong $^5A_1$ complex bands slightly shifted at 1523.6 and 1108.0 cm^{-1} as before but also weaker HD counterparts at 1576.5 and 1133.4 cm^{-1} (Figure 6). In like fashion, the HD experiments give the latter bands but also weaker bands at 1524.1 and 1108.2 cm^{-1}. These slight shifts are due to small secondary isotopic effects from the complexing dihydrogen relative to the pure isotopic species. Of more importance is observation of the CrH_2 and CrD_2 complex bands using HD and the CrHD complex bands with H_2+D_2. This indicates isotopic exchange between the chromium dihydride and dihydrogen portions of the complex through a symmetrical energized $[CrH_4]^*$ intermediate produced in the initial reaction. When excited Cr forms $[CrH_2]^*$ and then the $[(D_2)CrH_2]^*$ complex, rearrangement to tetrahedral $[CrH_2D_2]^*$ follows, some of which can relax to the $^5A_1$ (HD)CrHD complex.

Note that the 1525.8 cm^{-1} band for $(H_2)CrH_2$ is substantially broader than the sharp 1627.7 cm^{-1} CrH_2 absorption in solid neon. This may arise from hindered rotation of (H_2) about the C_2 axis of the complex. The position of the (H_2) ligand in the $(H_2)CrH_2$ complex is not as precisely defined as the structure of the CrH_2 subunit.

$(H_2)_2CrH_2$. On further annealing the 1525.8 cm^{-1} neon matrix absorption decreases and a sharp 1529.5 cm^{-1} peak appears (Figure 4). Annealing with D_2 in solid neon transformed the initial 1107.6 cm^{-1} product to a sharp 1112.2 cm^{-1} peak (H/D ratio 1.3752). With HD in neon, annealing produced sharp peaks at 1583.4, 1530.9, 1137.1, and 1113.0 cm^{-1}, and almost identical sharp peaks formed at 1583.3, 1530.8, 1137.0, and 1112.8 cm^{-1} using H_2+D_2. These bands are due to CrHD, CrH_2, CrHD, and CrD_2 subunits, respectively, in a new complex. Accordingly we identify the linear CrH_2 subunit in the $^5A_1$ (H_2)-$CrH_2(H_2)$ complex, which we find by DFT to be the most stable form for CrH_6. Our calculations predict this strong b_2 mode 20 cm^{-1} above the b_2 mode for $(H_2)CrH_2$ and 133 cm^{-1} below the b_2 mode for CrH_2, which are in good agreement with the observed neon matrix bands.

In similar $W/H_2/Ne$ experiments, annealing increased WH_6 absorptions,[1] and we expect the CrH_6 stiochiometry to form in the present experiments. We have no absorptions in the 1800−2400 cm^{-1} region where $Cr(\eta^2\text{-}H_2)_3$ and trigonal CrH_6 are calculated to have strong absorptions (Table 3). Hence, the present experiments provide strong evidence for the formation of CrH_6 here in the nearly planar bis dihydrogen complex (H_2)-$CrH_2(H_2)$ structure.

Pure hydrogen and deuterium gave strong 1521.3 and 1106.9 cm^{-1} bands (ratio 1.3744) whereas pure HD gave strong 1574.2 and 1131.7 cm^{-1} absorptions (ratio 1.3910) and weaker 1522.8 and 1107.9 cm^{-1} absorptions (ratio 1.3745). Mixtures of H_2 and D_2 produced new split absorptions in the 1523 and 1107 cm^{-1} regions, and the important conclusion is that these CrH_2 and CrD_2 stretching modes exhibit sufficient splittings to require more than one (namely two) perturbing dihydrogen ligands. The strongest 1523.5 cm^{-1} band increases with H_2 percentage and is probably due to $(H_2)_2CrH_2$ in the H_2/D_2 matrix which is 2.2 cm^{-1} higher than in pure H_2. The 1525.4 and 1521.9 cm^{-1} bands increase on photolysis and decrease on annealing: 1579.3 and 1574.2 cm^{-1} bands also increase on photolysis in the CrHD stretching region. Accordingly, the 1525.4 cm^{-1} band involves an HD ligand and is probably due to $(HD)(H_2)CrH_2$, and the 1521.9 cm^{-1} band is likely due to $(D_2)(H_2)CrH_2$. With pure HD the 1522.8 cm^{-1} band is due to $(HD)_2CrH_2$. Exchange between the dihydrogen ligand and matrix cage apparently occurs on annealing. Exchange also occurs between the dihydride and

dihydrogen ligand as weaker $(L)_2CrHD$ bands are observed with H_2/D_2 and weaker $(L_2)CrH_2$, $(L)_2CrD_2$ absorptions are formed in pure HD.

In an early investigation of reactions of Cr with H_2 in krypton and argon matrices, strong absorptions at 1510.5 cm^{-1} (Kr) and 1513.0 cm^{-1} (Ar) were observed.[10] Based on isotopic shift patterns these bands were assigned to chromium trihydride CrH_3. Later ab initio frequency calculations predicted the ν_3 mode for CrH_3 to be 200 cm^{-1} higher than the experimental assignment,[12] and the same result is found by our theoretical calculations. The observed bands at 1510.5 cm^{-1} (Kr) and 1513.0 cm^{-1} (Ar) are probably due to the higher $(H_2)_2CrH_2$ complex described here.

Polynuclear Chromium Hydrides. The most prominent band at 1335.0 cm^{-1} in the lower frequency region increases on photolysis as does the 1525.4 cm^{-1} $(H_2)CrH_2$ absorption. However the 1335.0 cm^{-1} band increases markedly (from 1/9 to 1/3 to 2/3) relative to the 1525.4 cm^{-1} band with increasing laser energy (Figure 7), which increases the Cr atom concentration. Two other bands at 1244.0 and 569.8 cm^{-1} track with the strong 1335.0 cm^{-1} band. The strong deuterium counterpart at 971.6 cm^{-1} has associated bands at 1148.8 cm^{-1} at 932.6 cm^{-1}. These bands are found at 1144.8, 971.2, and 931.2 cm^{-1} in pure deuterium and at 1578.4 and 1336.6 cm^{-1} in pure hydrogen. The dihydrogen counterpart for the 1148.8 cm^{-1} band is predicted under water, and growth of a 1599 cm^{-1} shoulder absorption is in accord.

Since CrH_2 is the major primary product, calculations were done for $(CrH_2)_2$, and the most stable isomer located is the distorted rhombus (C_{2h}) structure in Figure 10. Notice that this structure is a confederation of CrH_2 subunits. The strongest frequencies predicted at 1672.5, 1364.8, and 1134.9 cm^{-1} are in the region of the strongest bands observed here. The agreement is acceptable considering the difficulties in modeling a high-spin dichromium species.

Other dichromium species are observed in this region. The tracking bands at 1377.7 and 1299.9 cm^{-1} (D_2 counterparts at 994.2 and 950.0 cm^{-1}) are due to a dihydride subunit in a larger molecule that cannot be identified. We find no evidence for bridging hydrogen vibrations, computed in the 800−1100 cm^{-1} region. However, the high-spin $(CrH)_2$ dimer predicted to absorb strongly at 1097.4 cm^{-1} might complex dihydrogen and shift into the region of observed absorptions.

Reactions of Cr atoms in Solid Ar, Ne, Hydrogen, and Deuterium. The CrH and CrH_2 absorptions are produced only on deposition or sample photolysis, and they do not increase on annealing, suggesting that reactions of chromium atoms with H_2 are endothermic and activation energy is required. Our B3PW91 calculations predict that both reactions 1 and 2 are endothermic. Hence, energetic laser-ablated Cr atoms have sufficient excess energy to activate the H−H bond and give the CrH and CrH_2 products, which have been trapped in low-temperature matrix samples. Considerable excess kinetic energy is available in laser-ablated metal atoms,[37] and there are a host of excited Cr metastable electronic states[38] that can activate reactions 1 and 2. Reaction 2 is also promoted by $\lambda > 380$ nm radiation, which likely provides the z $^7P_4$ excited state (425 nm) of Cr for immediate reaction with H_2.

$$Cr(^7S_3) + H_2 \rightarrow CrH(^6\Sigma^+) + H \quad \Delta E = 54.0 \text{ kcal/mol} \quad (1)$$

$$Cr(^7S_3) + H_2 \rightarrow CrH_2\,(^5B_2) \quad \Delta E = 10.2 \text{ kcal/mol} \quad (2)$$

The CrH species is very reactive and rapidly combines with H_2 on annealing to give the $(H_2)CrH$ complex, reaction 3, which is slightly exothermic, and no activation energy is required. However this reaction is reversed by broadband photolysis in solid argon (Figures 1,2). Recall that $(H_2)CrH$ is more stable than CrH_3, and CrH_3 is not observed in these experiments.

$$CrH(^6\Sigma^+) + H_2 \rightarrow (H_2)CrH\,(^6A_1) \quad \Delta E = -1.2 \text{ kcal/mol (B3PW91)} \quad (3)$$

Likewise CrH_2 is coordinated by H_2 to form $(H_2)CrH_2$ and $(H_2)_2CrH_2$ species, and the latter is favored in pure hydrogen. Ma et al. point out that bent ground-state CrH_2 ($^5B_2$) is weakly repulsive to one H_2 molecule, but that the linear $^5A_1$ excited state does attract H_2 and that CrH_4 ($^3A_1$) is 38.5 kcal/mol higher in energy.[11b] Hence $(H_2)CrH_2$ and not CrH_4 is observed in these experiments. However, we find that two H_2 molecules are attractive to ground-state CrH_2, and the most stable CrH_6 structure, $(H_2)CrH_2(H_2)$, results on annealing solid neon to 12 K to allow diffusion and reaction of trapped H_2, reactions 5 and 6, which are exothermic (−4.1 and −4.2 kcal/mol, respectively) at the MP2 level of theory.

$$CrH_2(^5A_1) + H_2 \rightarrow (H_2)CrH_2\,(^5A_1) \quad \Delta E = -3.1 \text{ kcal/mol}^{11b} \quad (4)$$

$$CrH_2(^5B_2) + 2H_2 \rightarrow (H_2)_2CrH_2\,(^5A_1) \quad \Delta E = -0.2 \text{ kcal/mol (B3PW91)} \quad (5)$$

$$(H_2)CrH_2(^5A_1) + H_2 \rightarrow (H_2)_2CrH_2\,(^5A_1) \quad \Delta E = -7.2 \text{ kcal/mol (B3PW91)} \quad (6)$$

A difference between argon and neon is apparent here. Apparently, the excess energy imparted by laser-ablated Cr into the CrH_2 product of reaction 2 is efficiently relaxed by condensing argon so that only the weak $(H_2)-CrH_2$ ($^5B_2$) ground-state complex is formed, but in neon the stable product of excited CrH_2 ($^5A_1$) reaction 4, $(H_2)CrH_2$ is trapped. Hence condensing neon quenches excited CrH_2 less efficiently than condensing argon and allows the stable $(H_2)CrH_2$ complex to be formed.

It is interesting to note that the final stable structure formed on annealing for chromium hexahydride is CrH_2 coordinated by two H_2 ligands on opposite sides of linear CrH_2, which is the dominant product in pure hydrogen, and that CrH_6 lies higher in energy. Additional splittings in pure H_2/D_2 and pure HD experiments require two dihydrogen ligands. It appears that exchange occurs between the matrix cage and dihydrogen ligands on $(H_2)_2CrH_2$ in mixed pure H_2/D_2 experiments. A similar bis-dihydrogen complex has been observed for CrO_2, but the H_2 ligands are on the same side of the bent CrO_2 host molecule.[39] The distorted trigonal prism CrH_6 structure is 41.0 kcal/mol higher at the MP2 level, and the tris-dihydrogen complex $Cr(\eta^2\text{-}H_2)_3$ is 53.3 kcal/mol higher at the B3PW91 level. For these higher energy CrH_6 species, MP2 finds stronger binding of hydrogen and more elongation of the H−H′ reagent bonds (Table 2), which is in accord with findings for other complexes.[34,35]

We found isotopic scrambling in $(H_2)CrH_2$ (and $(H_2)_2CrH_2$) on deposition and on ultraviolet photolysis, which provide energetic Cr atoms for reaction. This means that sufficient excess energy is available to produce the excited $[CrH_4]^*$ species on the triplet potential surface where all atomic positions are equivalent. The $[CrH_2D_2]^*$ intermediate can be formed from H_2+D_2 and from 2 HD molecules, and when $[CrH_2D_2]^*$ is relaxed all three complexes (HD)CrHD, $(H_2)CrD_2$, and (D_2)-CrH_2 are trapped. Similar isotopic scrambling has been observed

for rhodium and group 3 transition metal hydrides.[23,40]

$$Cr^* + H_2 + D_2 \rightarrow [CrH_2D_2]^* \xrightarrow{\text{relax}} (HD)CrHD \quad (7a)$$

$$\rightarrow (H_2)CrD_2 \quad (7b)$$

$$\rightarrow (D_2)CrH_2 \quad (7c)$$

Evidence is presented for dichromium species, and the $(CrH_2)_2$ dimer is more stable than two CrH_2 molecules by 28.9 kcal/mol.

$$2CrH_2(^5B_2) \rightarrow Cr_2H_4(^9A_g)$$

$$\Delta E = -28.9 \text{ kcal/mol (B3PW91)} \quad (8)$$

Conclusions

Laser-ablated Cr atoms react with H_2 to give CrH and CrH_2 as primary products, which react further with H_2 to produce the $(H_2)CrH$, $(H_2)CrH_2$, and $(H_2)_2CrH_2$ complexes in solid argon, neon, hydrogen, and deuterium matrices. Absorption for (H_2)-CrH at 1547.5 cm^{-1} in argon is the major product: this absorption shifts to 1561.8 cm^{-1} in neon and to 1119.0 cm^{-1} in deuterium. A weak $(H_2)-CrH_2$ complex involving $^5B_2$ ground-state CrH_2 is observed at 1581.3 cm^{-1} in argon, and a strong $(H_2)CrH_2$ complex ($^5A_1$) in neon at 1525.4 cm^{-1}. A major absorption at 1529.5 cm^{-1} after annealing in neon is due to $(H_2)_2CrH_2$, the bis-dihydrogen complex, which is the most stable form for CrH_6. This complex is observed at 1521.3 cm^{-1} in pure hydrogen and at 1106.9 cm^{-1} in pure deuterium as $(D_2)_2$-CrD_2. The trend of dihydrogen complex structure for $(H_2)_2CrH_2$ to hydride structure[1] for WH_6 is observed for other groups.[34]

The $(H_2)CrH$ complex with lower energy compared to CrH_3 is trapped in matrices and no band is observed for CrH_3. This result is in accord with recent theoretical investigations[11b,12] and requires reassignment of bands in an earlier matrix isolation study.[10] Likewise $(H_2)CrH_2$ is lower in energy than CrH_4, and accordingly $(H_2)CrH_2$ is observed here although the excited $[CrH_2D_2]^*$ intermediate plays a role in isotopic scrambling. The most stable structure for chromium hexahydride is the bis-dihydrogen complex, $(H_2)_2CrH_2$, which has been identified by isotopic substitution on the matrix infrared spectrum and theoretical investigations (DFT and MP2).

Acknowledgment. We gratefully acknowledge support for this work from N.S.F Grant CHE 00-78836 and helpful discussions with O. Eisenstein.

References and Notes

(1) Wang, X.; Andrews, L. *J. Am. Chem. Soc.* **2002**, *124*, 5636. *J. Phys. Chem. A* **2002**, *106*, 6720 (W+H_2).
(2) Huber, K. P.; Herzberg, G. *Molecular Spectra and Molecular Structure, Vol. IV, Constants of Diatomic Molecules*; Van Nostrand Reinhold: New York, 1979.
(3) Chong, D. P.; Langhoff, S. R.; Bauschlicher, C. W., Jr.; Walch, S. P.; Partridge, H. *J. Chem. Phys*. **1986**, *85*, 2850.
(4) Lipus, K.; Bachem, E.; Urban, W. *Mol. Phys.* **1991**, *73*, 1041.
(5) Corkery, S. M.; Brown, J. M.; Beaton, S. P.; Evenson, K. M. *J. Mol. Spectrosc*. **1991**, *149*, 257.
(6) Dai, D.; Balasubramanian, K. *J. Mol. Spectrosc*. **1993**, *161*, 455.
(7) (a) Ram, R. S.; Jarman, C. N.; Bernath, P. F. *J. Mol. Spectrosc*. **1993**, *161*, 445. (b) Ram, R. S.; Bernath, P. F. *J. Mol. Spectrosc*. **1995**, *172*, 91.
(8) Bauschlicher, C. W., Jr.; Ram, R. S.; Bernath, P. F.; Parsons, C. G.; Galehouse, D. *J. Chem. Phys*. **2001**, *115*, 1312.
(9) Van Zee, R. J.; DeVore, T. C.; Weltner, W., Jr. *J. Chem. Phys*. **1979**, *71*, 2051.
(10) Xiao, Z. L.; Hauge, R. H.; Margrave, J. L. *J. Phys. Chem*. **1992**, *96*, 636.
(11) (a) Deleeuw, B. J.; Yamaguchi, Y.; Schaefer, H. F., III *Mol. Phys*. **1995**, *84*, 1109. (b) Ma, B.; Collina, C. L.; Schaefer, H. F., III *J. Am. Chem. Soc.* **1996**, *118*, 870.
(12) Balabanov, N. B.; Boggs, J. E. *J. Phys. Chem. A* **2000**, *104*, 7370.
(13) (a) Kang, S. K.; Albright, T. A.; Eisenstein, O. *Inorg. Chem*. **1989**, *28*, 1611. (b) Kang, S. K.; Tang, H.; Albright, T. A. *J. Am. Chem. Soc*. **1993**, *115*, 1971.
(14) Shen, M.; Schaefer, H. F., III; Partridge, H. *J. Chem. Phys*. **1993**, *98*, 508.
(15) Tanpipat, N.; Baker, J. *J. Phys. Chem*. **1996**, *100*, 19818.
(16) Kaupp, M. *J. Am. Chem. Soc*. **1996**, *118*, 3018.
(17) Andrews, L.; Wang, X.; Manceron, L. *J. Chem. Phys*. **2001**, *114*, 1559 (Pt + H_2).
(18) Andrews, L.; Manceron, L.; Alikhani, M. E.; Wang, X. *J. Am. Chem. Soc*. **2000**, *122*, 11011.
(19) Andrews, L.; Wang, X.; Alikhani, M. E.; Manceron, L. *J. Phys. Chem.* A **2001**, *105*, 3052 (Pd+H_2).
(20) Chertihin, G. V.; Andrews, L. *J. Am. Chem. Soc*. **1994**, *116*, 8322 (Ti+H_2).
(21) Chertihin, G. V.; Andrews, L. *J. Am. Chem. Soc*. **1995**, *117*, 6402 (Zr, Hf+H_2).
(22) Chertihin, G. V.; Andrews, L. *J. Phys. Chem*. **1995**, *99*, 15004 (Zr, Hf+H_2).
(23) Wang, X.; Andrews, L. *J. Phys. Chem. A* **2002**, *106*, 3706 (Rh+H_2).
(24) (a) Wang, X.; Andrews, L. *J. Am. Chem. Soc*. **2001**, *123*, 12899. (b) Wang, X.; Andrews, L. *J. Phys. Chem. A* **2002**, *106*, 3744 (Au+H_2).
(25) Burkholder, T. R.; Andrews, L. *J. Chem. Phys*. **1991**, *95*, 8697.
(26) Hassanzadeh, P.; Andrews, L. *J. Phys. Chem*. **1992**, *96*, 9177.
(27) Zhou, M.; Andrews, L. *J. Chem. Phys*. **1999**, *111*, 4230 (Cr+O_2).
(28) Frisch, M. J.; Trucks, G. W.; Schlegel, H. B.; Scuseria, G. E.; Robb, M. A.; Cheeseman, J. R.; Zakrzewski, V. G.; Montgomery, J. A., Jr.; Stratmann, R. E.; Burant, J. C.; Dapprich, S.; Millam, J. M.; Daniels, A. D.; Kudin, K. N.; Strain, M. C.; Farkas, O.; Tomasi, J.; Barone, V.; Cossi, M.; Cammi, R.; Mennucci, B.; Pomelli, C.; Adamo, C.; Clifford, S.; Ochterski, J.; Petersson, G. A.; Ayala, P. Y.; Cui, Q.; Morokuma, K.; Malick, D. K.; Rabuck, A. D.; Raghavachari, K.; Foresman, J. B.; Cioslowski, J.; Ortiz, J. V.; Stefanov, B. B.; Liu, G.; Liashenko, A.; Piskorz, P.; Komaromi, I.; Gomperts, R.; Martin, R. L.; Fox, D. J.; Keith, T.; Al-Laham, M. A.; Peng, C. Y.; Nanayakkara, A.; Gonzalez, C.; Challacombe, M.; Gill, P. M. W.; Johnson, B.; Chen, W.; Wong, M. W.; Andres, J. L.; Gonzalez, C.; Head-Gordon, M.; Replogle, E. S.; Pople, J. A. *Gaussian 98*, Revision A.6; Gaussian, Inc.: Pittsburgh, PA, 1998.
(29) (a) Krishnan, R.; Binkley, J. S.; Seeger, R.; Pople, J. A. *J. Chem. Phys*. **1980**, *72*, 650. (b) Frisch, M. J.; Pople, J. A.; Binkley, J. S. *J. Chem. Phys*. **1984**, *80*, 3265.
(30) Leininger, T.; Nicklass, A.; Stoll, H.; Dolg, M.; Schwerdtfeger, P. *J. Chem. Phys*. **1996**, *105*, 1052.
(31) Becke, A. D. *Phys. Rev. A* **1988**, *38*, 3098. Perdew J. P. *Phys. Rev. B* **1983**, *33*, 8822. Perdew, J. P.; Wang, Y. *Phys. Rev. B* **1992**, *45*, 13244.
(32) Becke, A. D. *J. Chem. Phys*. **1993**, *98*, 5648. Stevens, P. J.; Devlin, F. J.; Chablowski, C. F.; Frisch, M. J. *J. Phys. Chem*. **1994**, *98*, 11623.
(33) Mϕller, C.; Plesset, M. S. *Phys. Rev.* **1934**, *46*, 618.
(34) Maseras, F.; Lledos, A.; Clot, E.; Eisenstein, O. *Chem. Rev.* **2000**, *100*, 601.
(35) Clot, E.; Eisenstein, O. *J. Phys. Chem. A* **1998**, *102*, 3592.
(36) Jacox, M. E. *Chem. Phys*. **1994**, *189*, 149.
(37) Kang, H.; Beauchamp, J. L. *J. Phys. Chem.* **1985**, *89*, 3364.
(38) Moore, C. E. *Atomic Energy Levels, Vol. II.*; National Bureau of Standards: Gaithersburg, MD, 1952.
(39) Zhou, M.; Zhang, L.; Shao, L.; Wang, W.; Fan, K.; Qin, Q. *J. Phys. Chem. A* **2001**, *105*, 10747.
(40) Wang, X.; Andrews, L. *J. Am. Chem. Soc*. **2002**, *124*, 7610.